MOLECULAR AND CELLULAR BIOLOGY, Feb. 1997, p. 963–976 Vol. 17, No. 2
0270-7306/97/$04.00+0

AP-1-Mediated Invasion Requires Increased Expression of the Hyaluronan Receptor CD44

RICHARD F. LAMB, ROBERT F. HENNIGAN,† KENNETH TURNBULL, KOSTAS D. KATSANAKIS, ELAINE D. MACKENZIE, GEORGE D. BIRNIE, AND BRADFORD W. OZANNE*

CRC Beatson Laboratories, Beatson Institute for Cancer Research, Bearsden, Glasgow, Scotland

Received 23 May 1996/Returned for modification 12 July 1996/Accepted 18 October 1996

Fibroblasts transformed by Fos oncogenes display increased expression of a number of genes implicated in tumor cell invasion and metastasis. In contrast to normal 208F rat fibroblasts, Fos-transformed 208F fibroblasts are growth factor independent for invasion. We demonstrate that invasion of v-Fos- or epidermal growth factor (EGF)-transformed cells requires AP-1 activity. v-Fos-transformed cell invasion is inhibited by c-*jun* antisense oligonucleotides and by expression of a c-*jun* dominant negative mutant, TAM-67. EGF-induced invasion is inhibited by both c-*fos* and c-*jun* antisense oligonucleotides. CD44s, the standard form of a transmembrane receptor for hyaluronan, is implicated in tumor cell invasion and metastasis. We demonstrate that increased expression of CD44 in Fos- and EGF-transformed cells is dependent upon AP-1. CD44 antisense oligonucleotides reduce expression of CD44 in v-Fos- or EGF-transformed cells and inhibit invasion but not migration. Expression of a fusion protein between human CD44s and *Aequorea victoria* green fluorescent protein (GFP) in 208F cells complements the inhibition of invasion by the rat-specific CD44 antisense oligonucleotide. We further show that both v-Fos and EGF transformations result in a concentration of endogenous CD44 or exogenous CD44-GFP at the ends of pseudopodial cell extensions. These results support the hypothesis that one role of AP-1 in transformation is to activate a multigenic invasion program.

The proto-oncogene c-*fos* is the cellular homolog of the v-*fos* oncogenes carried by Finkel-Biskis-Jinkins (FBJ) and Finkel-Biskis-Reilly (FBR) murine sarcoma viruses. It belongs to a family of genes encoding nuclear transcription factors implicated in orchestrating cell growth and differentiation that include *fra*-1 (16), *fra*-2 (62), and *fos*B (86). These proteins are thought to mediate their cellular functions by forming heterodimers with members of the Jun family of nuclear oncoproteins that include c-*jun* (61), *jun*B (67), and *jun*D (31, 68) to form the transcription factor activator protein 1 (AP-1). Transient induction of c-*fos* and AP-1 DNA-binding activity results from activation of signal transduction pathways which transduce signals from the cell membrane to the nucleus (18). Mutational activation of proto-oncogenes such as *sis*, *ras*, and *raf* that participate in such pathways results in deregulated expression of c-*fos* (38, 46, 74) and an increase in AP-1 activity that is necessary for transformation by these oncogenes (76). Although the induction of AP-1 activity in fibroblasts by a variety of stimuli, including serum (22, 27), cytokines (11), tumor promoters (3), and growth factors (15), implicates AP-1 activation in the regulation of proliferation, this may not be its only contribution to transformation. Inhibition of AP-1 activity also blocks morphological transformation by oncogenes that lie upstream of c-*fos* (47). Similarly, v-*fos*-transformed cells express the transformed morphology while remaining dependent upon serum mitogens for proliferation (27, 30, 55). Moreover, fibroblast cell lines from c-*fos*-null mice display a normal dependence on serum mitogens for proliferation and normal expression of several genes containing functional AP-1 sites in their promoters (13, 34). In such cells, however, expression of two genes, those for stromelysin 1 and type 1 collagenase, normally upregulated in transformed cells or by growth factors, is severely attenuated (34). Thus, although AP-1 regulates the expression of a diverse group of genes, including c-*jun* (4), MCP-1 (66), those for metalloproteases stromelysin 1 and type 1 collagenase (42, 72), those for metallothionines (44), and that for CD44 (32), c-*fos* expression may be required only for a subset of these. Two examples of c-*fos*-requiring genes, those for type 1 collagenase and stromelysin 1, encode proteases involved in degradation of extracellular matrix (ECM). Expression of these genes is induced both in Fos-transformed cells that can invade ECM in vitro (30) and in normal stromal fibroblasts invading in response to epidermal wounding (21), consistent with the idea that *fos* may play a pivotal role in regulating genes involved in invasion (30).

The cell surface hyaluronan receptor CD44s is expressed in a variety of normal tissues and tumors. CD44s belongs to a family of structurally related transmembrane proteins with a common cytoplasmic tail domain (35). Variants of CD44 differ from CD44s as a result of alternative splicing and posttranslational modification in the extracellular domain of the molecule (28). An association between overexpression of CD44s or alternatively spliced variants with aggressiveness or metastasis of a variety of human tumors (51, 58) suggests that these proteins play a role in tumor progression. This is supported by the findings that CD44 has a role in tumor cell motility in vitro (8, 19, 79) and enhances tumor growth and metastasis in in vivo models (25, 26). Interaction of CD44s with the ECM proteoglycan hyaluronan appears to be one key aspect of its function (5, 17, 57) and is critical for CD44s to promote melanoma tumor development (6). However, CD44 has also been shown to interact with other ECM components (7, 36, 85) and to promote cell-cell adhesion (75). In fibroblasts the CD44 promoter is AP-1 responsive (32) and CD44 expression is upregulated in cells transformed by either v-*src* or activated H-*ras* (32,

* Corresponding author. Mailing address: Beatson Institute for Cancer Research, CRC Beatson Laboratories, Garscube Estate, Switchback Rd., Bearsden, Glasgow G61 1BD, Scotland. Phone: 0141-942-9361. Fax: 0141-942-6521. E-mail: gpma15@udcf.gla.ac.uk.

† Present address: Department of Cell Biology, Neurobiology and Anatomy, University of Cincinnati College of Medicine, Cincinnati, Ohio.

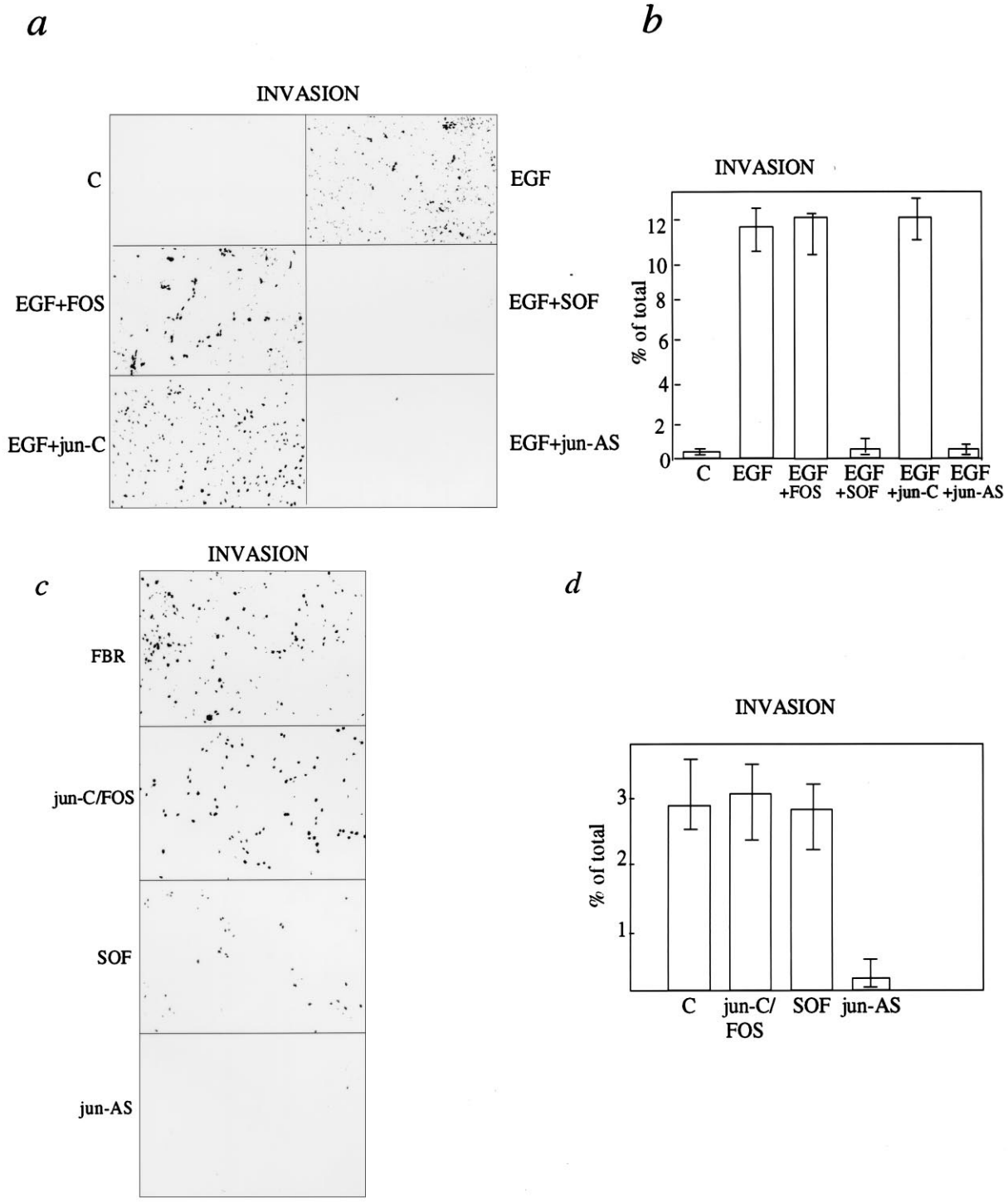

FIG. 1. Antisense oligonucleotide to AP-1 components inhibits v-*fos*- or EGF-induced 208F ECM invasion. (a) 208F invasion in response to EGF. Shown are confocal images of propidium iodide-stained cell nuclei at 20 μm in Matrigel of 208F in the absence (C) or presence (EGF) of EGF alone or in the presence of control (EGF+jun-C) or antisense (EGF+jun-AS) c-*jun* or sense (EGF+FOS) or antisense (EGF+SOF) c-*fos* phosphorothioate oligonucleotide. (b) Quantitative analysis of invasion. Invasion assay results were quantitated as described elsewhere (30) with a Bio-Rad program (Comos) and represent the average from at least four separate assays in two experiments. (c) FBR v-*fos* invasion. Shown are confocal images of propidium iodide-stained cell nuclei at 20 μm in Matrigel of FBR v-*fos* in the absence (FBR) or presence of control and sense (jun-C/FOS) or anti-c-*jun* (jun-AS) or -c-*fos* (SOF) phosphorothioate oligonucleotides. (d) Quantitative analysis of invasion. Invasion assay results were quantitated as in panel b.

37), which suggests that CD44 expression is normally regulated by signalling pathways in which these oncogenes participate.

A search designed to isolate AP-1 target genes upregulated in FBR v-*fos*-transformed cells identified a number of genes that have been implicated in invasion or metastasis (30). These included proteases involved in ECM degradation which are upregulated by *fos* or v-*ras* (52, 81) and induced in stromal fibroblasts during tissue remodeling (2, 21). Other genes iso-

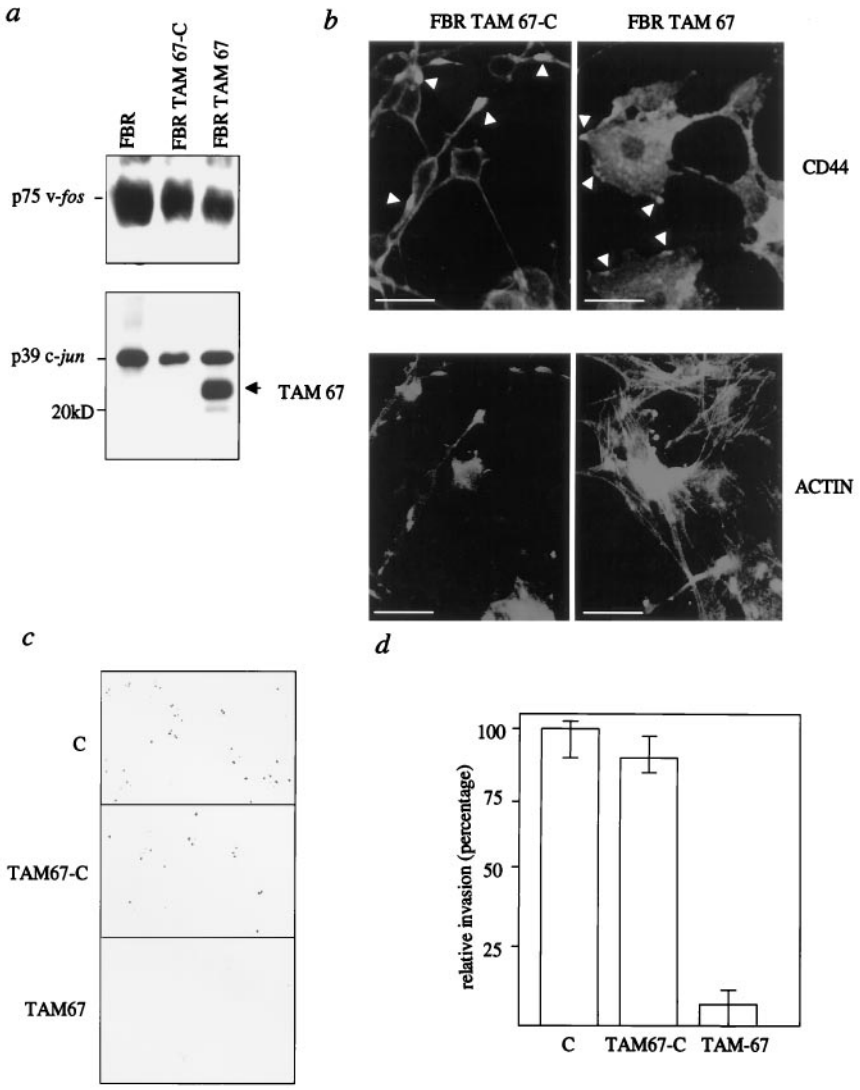

FIG. 2. Expression of dominant negative c-*jun* (TAM-67) inhibits invasion of FBR v-*fos*. (a) Immunoblot analysis of v-*fos* and c-*jun* TAM-67 in FBR cells or two G418^r FBR transfectants, transfected with Neo^r plasmid alone (FBR TAM-C) or cotransfected with TAM-67 expression plasmid (FBR TAM-67). v-*fos* and c-*jun* were detected with anti-pan-*fos* (Upstate Biotechnology) and AB-1 (Oncogene Science) antisera, respectively. (b) Morphological characteristics of TAM-67-expressing FBR. CD44 immunostaining (top) and phalloidin staining (bottom) in FBR TAM-C and FBR TAM-67 are shown. Anti-CD44 MAb OX49 was used to detect CD44. Concentrations of CD44 immunostaining are indicated by arrowheads. Bars, 25 μm. (c) Invasion of TAM-67-expressing FBR cells. Confocal images of propidium iodide-stained cell nuclei at 20 μm in Matrigel of FBR v-*fos* (C) or vector-transfected (TAM67-C) or TAM-67-expressing (TAM67) transfectants are shown. (d) Quantitative analysis of invasion of FBR, FBR TAM-C, or TAM-67-expressing transfectants. Invasion assay results were quantitated as in Fig. 1b. Invasion of FBR TAM-C or TAM-67 is expressed as a percentage of FBR invasion (100%).

lated have similarly been implicated in adhesion, motility, and metastasis (30, 40). Previously, we demonstrated that Fos-transformed cells are constitutively invasive, while normal cells require growth factors to stimulate invasion (30).

On the basis of the functions of the genes found to be upregulated as a consequence of v-*fos* transformation, we proposed that one role of AP-1 in transformation is to activate a multigenic invasion program. Herein we test two predictions which flow from this proposal. First, we show that invasion is dependent upon the expression of functional AP-1 in FBR v-*fos*-transformed 208F fibroblasts (FBR cells) or epidermal growth factor (EGF)-induced invasion of 208F fibroblasts. Second, we demonstrate that invasion of FBR or EGF-transformed 208F fibroblasts (41, 63) is dependent upon the increased expression of a known AP-1 target gene, CD44 (32). The results presented indicate a functional link between AP-1, CD44 induction, and in vitro ECM invasion.

MATERIALS AND METHODS

Human recombinant EGF was obtained from Life Technologies, Paisley, United Kingdom. Texas red (TRIC)-labelled phalloidin, fluorescein isothiocyanate (FITC)- and TRIC-labelled anti-mouse and FITC-labelled anti-rabbit immunoglobulin G (IgG), and propidium iodide were purchased from Sigma Chemical Co., Poole, United Kingdom. Antibodies used were anti-CD44 monoclonal antibodies (MAbs) 5G8 (used for Western blotting) (a generous gift from J. Sleeman, Institut für Genetik, Karlsruhe, Germany), OX49 (used for indirect immunofluoresence) (Serotech, Kidlington, United Kingdom), and Hermes-3 (used to detect human CD44) (a gift from E. Butcher, Department of Pathology, Stanford University Medical Center, Stanford, Calif.). Antivinculin and antitalin MAbs used as a loading controls in Western blotting were purchased from Sigma Chemical Co. Anti-green fluorescent protein (GFP) polyclonal serum was purchased from Clontech Laboratories, Palo Alto, Calif. Antibodies used to detect

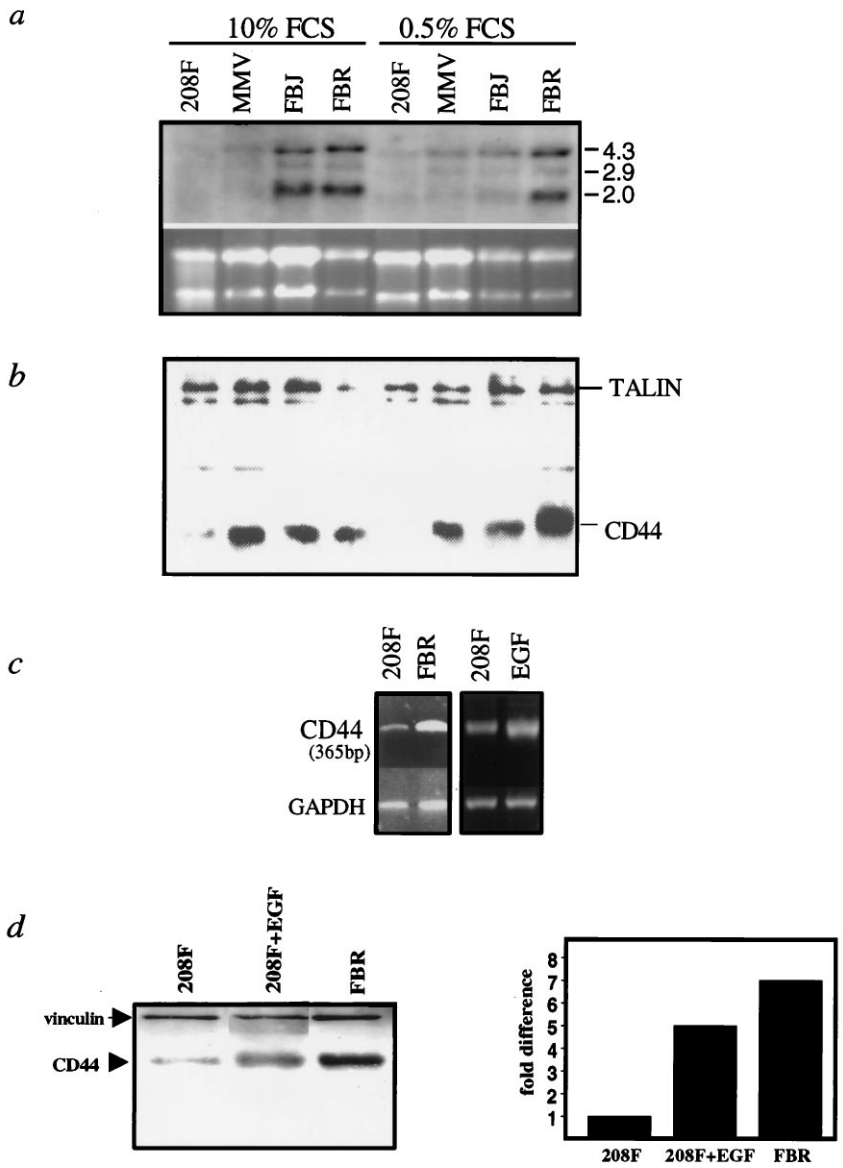

FIG. 3. CD44 upregulation in *fos* transformants and by EGF. (a) Northern analysis of CD44 mRNAs in c-*fos* transformant MMV, v-*fos* transformants FBJ and FBR, and normal 208F fibroblasts in growing (10% FCS) or growth-arrested (0.5% FCS) cultures. An ethidium bromide-stained gel prior to transfer is also shown to verify equal RNA loading. CD44 mRNA sizes (given in kilobases) were estimated relative to an RNA marker ladder (Life Technologies). (b) Western analysis of CD44 levels in *fos* transformants and 208F. Blots were probed with antibodies to talin and CD44 as described in Materials and Methods. CD44 is detected as an 85-kDa band with anti-CD44 MAb 5G8 in both v- and c-*fos* transformants. The two molecular weight size markers shown were from Life Technologies. (c) Semiquantitative RT-PCR of CD44 mRNAs. CD44 is upregulated in v-*fos* transformant FBR cells and in EGF-transformed 208F cells compared to untreated 208F. This 365-bp species lacking alternatively spliced exons is 5- to 10-fold more adundant in FBR cells or after EGF treatment. (d) Western analysis showing the relative adundance of p85 CD44s in 208F, 208F morphologically transformed by EGF treatment for 48 h, and v-*fos* FBR. Blots were probed as described above with 5G8 and antivinculin MAb to control for loading variations and transfer. Positions of molecular weight markers (Life Technologies) are also shown.

c-*jun*/TAM-67 (anti-c-*jun* AB-1) and v-*fos* (anti-pan *fos* K-25) were obtained from Oncogene Science, Cambridge, United Kingdom, and Santa Cruz Biotechnology, Santa Cruz, Calif., respectively. In vitro invasion chambers (Transwell; 8-μm-pore-size filter) were purchased from Costar. Reduced-growth-factor Matrigel was from Collaborative Research.

Cell lines. 208F is a subclone of the Rat-1 fibroblast line originally obtained from K. Quade. MMV is a constitutive c-*fos*-expressing cell line generated by transfection of 208F with murine c-*fos* lacking 5′ untranslated sequences and under the control of Rous sarcoma virus long-terminal repeat (56). v-*fos* transformants FBR and FBJ were originally obtained from Tom Curran and are nonproducer 208F fibroblasts transformed by infection with the FBR and FBJ murine sarcoma retroviruses, respectively. All cell lines were routinely passaged before confluence and maintained in Dulbecco modified Eagle medium (DMEM) (Life Technologies) supplemented with 10% fetal calf serum (FCS) (Advanced Protein Products Ltd.) at 37°C in 5% CO_2.

cDNA expression vectors and transfections. pSRαneo and pSRαneoCD44s, a construct expressing human CD44s, were kind gifts from C. M. Isacke, Imperial College, London, United Kingdom (59). A TAM-67 expression construct expressing a c-*jun* deletion mutant under the control of a cytomegalovirus promoter was a kind gift from Michael Birrer (12) and cotransfected in a 10:1 mixture with pSRαneo. 208F and FBR cells were transfected by lipofection (*N*-[1-(2,3-dioleoyloxylpropyl]-*N*,*N*,*N*-trimethylammonium methylsulfate [DOTAP; Life Technologies]) with 10 μg of cesium chloride-purified plasmid according to a protocol suggested by the manufacturer. After 10 to 14 days individual clones resistant to 300 μg of G418 per ml were obtained and subcloned by limiting dilution to generate single-cell subclones. At least 10 to 15 subclones were obtained for each transfection and examined by epifluorescence of live cells (for GFP and CD44-GFP fluoresence) or Western blotting (for TAM-67 expression) and by both Western blotting and indirect immunofluoresence with anti-human CD44-specific antiserum (Hermes-3) for human CD44 and CD44-GFP fusion

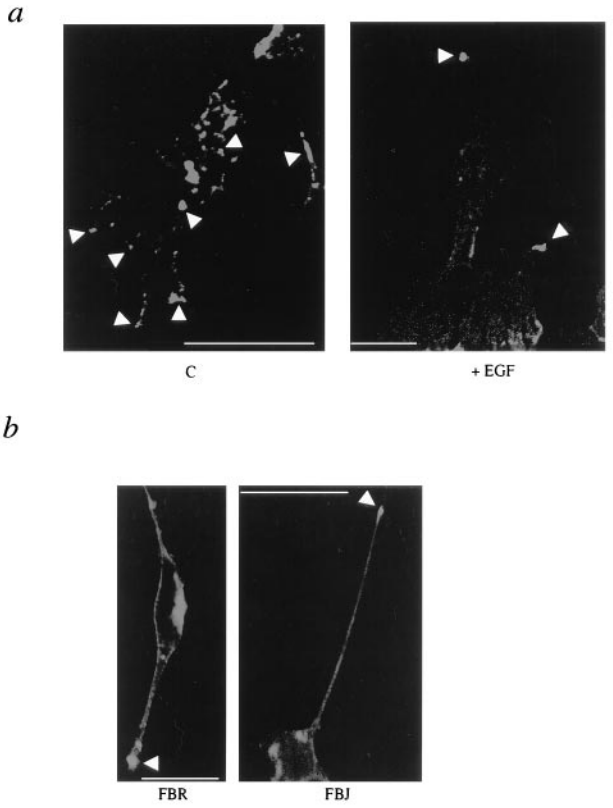

FIG. 4. CD44 immunolocalization in 208F, EGF-transformed 208F, and v-*fos* transformants. (a) Morphological transformation of 208F by EGF. CD44 immunostaining (with OX49 MAb) of 208F in the absence (C) or presence (+EGF) of 40 ng of EGF per ml for 48 h is shown. Note the elongated morphology after treatment with EGF. CD44 immunolocalizes at microvilli and membrane ruffles in untreated 208F (arrowheads) and is concentrated at pseudopodial tips (arrowheads) in EGF-treated cells. (b) CD44 immunolocalization (with anti-rat CD44 MAb OX49) in v-*fos* transformants. Note the concentration of CD44 immunostaining at pseudopodial tips (arrowheads) in both FBR and FBJ v-*fos* transformants. Bars, 25 μm.

and anti-GFP antiserum for CD44-GFP fusion and GFP. For transient transfection of GFP or CD44-GFP, cells grown on chamber slides (Costar) or 9-cm-diameter dishes were lipofected as described above with 30 μg of plasmid DNA, allowed to express the transfected DNA for 2 days, and either maintained in growth medium or transformed by treatment with EGF as described below.

Construction and expression of CD44-GFP fusion. A C-terminal fusion of human CD44s with the S65T mutant (29) of the *A. victoria* GFP was generated as follows: a plasmid encoding full-length human CD44 (pSRαneoCD44) was subjected to PCR with oligonucleotides C3 and C-FUS, where C-FUS lacks the termination codon of human CD44, instead creating a C-terminal *Not*I site (underlined): C3, GGA TCC TCC AGC TCC TTT CG; C-FUS, ACGT GCG GCCGC CAC CCC AAT CTT CAT GTC CAC ATT C.

PCR was performed with a Perkin-Elmer DNA Thermal Cycler 480 under the following cycle conditions: 1 min at 93°C, 1 min at 55°C, and 2 min at 73°C for 25 cycles with 100 ng of each oligonucleotide and 5 ng of denatured pSRαneoCD44. The 1.1-kb fragment was purified and blunt end ligated into *Bam*HI-digested and blunted pSRαneo as described elsewhere (59), generating the intermediate construct pSRαneoCD44C-FUS. The correct 5′-3′ orientation of the CD44 fragment with respect to the pSRα promoter was confirmed by restriction endonuclease digestion. An in-frame fusion of CD44 with GFP was generated with a plasmid encoding the S65T mutant of GFP (29) in the eukaryotic expression vector pCMX (a kind gift from Jonathon Pines). GFP lacking the initiation codon was generated by PCR using the following oligonucleotides: N-FUS, ACG TGC GGC CGC T AGT AAA GGA GAA GAA CTT TTC ACT; 3′GFP, ACG TGC GGC CGC GAT CCT CTA GCT ACC TAG CTA GCT.

PCR was performed as described above with *Pfu-Taq* and the 750-bp GFP fragment purified from PCR on a commercial spun-column chromatography column (Microspin S-300; Pharmacia), precipitated, and digested overnight with *Not*I (Boehringer Corp., London, Ltd., Lewes, United Kingdom). The *Not*I-digested GFP fragment was gel purified and ligated into the pSRαneoCD44C-FUS vector which had previously been digested with *Not*I and dephosphorylated by treatment with CIP (BCL). The construct containing the correct orientation of GFP was sequenced by dideoxy chain termination sequencing to confirm that an in-frame fusion of human CD44 (first set of boldfaced codons) with GFP (second set of boldfaced codons) had been generated: **GGG GTG** GCG GCC GCT **AGT AAA GGA** (Gly Val Ala Ala Ala Ser Lys Gly).

To generate a similar construct expressing only GFPS65T, the coding sequences of GFP in plasmid pCMX (above) were amplified by PCR with *Pfu-Taq* as described above with primers spanning the GFP coding sequences (data not shown). GFP was ligated into *Bam*HI-digested and blunted pSRαneo as described above, and correctly oriented clones were verified by restriction endonuclease digestion. Transfection of 208F with this expression construct verified GFP fluoresence in G418^r transfectants after visualization of live cells under UV illumination with a conventional FITC filter setting.

RT-PCR, Northern, and Western analyses. Semiquantitative reverse transcription (RT)-PCR was performed using 1 μg of total cellular RNA. Total RNA was prepared by RNAzol B extraction using a protocol supplied by the manufacturer (Biogenesis). cDNA syntheses using random hexamers and PCR were performed using a commercial RT-PCR kit (Perkin-Elmer) on a Perkin-Elmer DNA Thermal Cycler 480 under the following cycle conditions: one cycle of 5 min at 92°C, 5 min at 55°C, and 15 min at 73°C followed by 30 cycles of 1 min at 93°C, 1 min at 55°C, and 5 min at 73°C. A final elongation step of 15 min at 73°C was performed to complete synthesis. To standardize cDNA, primers from human glyceraldehyde-3-phosphate dehydrogenase (1) were used under the above-described cycle conditions. cDNA was then amplified with these primers and primers spanning the region of CD44 alternative splicing and corresponding to the following sequences in the common exons of rat CD44, with numbering corresponding to the published rat CD44 sequence (25): 5′ primer (bases 516 to 544), 5′-CAG TCA CAG ACC TAC CCA ATT CCT TCG AT-3′; 3′ primer (bases 1342 to 1370), 5′-CCA GGA GGG ATG CCA AGA TGA TAA GCC AC-3′. The 365-bp fragment amplified was confirmed to be derived from CD44 mRNA by Southern blot hybridization with CD44 oligonucleotides internal to the primers used for RT-PCR and by direct sequencing (data not shown).

For Northern analysis, 10 μg of total cellular RNA purified as for RT-PCR was separated on a 1% agarose–formaldehyde–MOPS (morpholinepropanesulfonic acid) gel (70). The RNA gel was stained with ethidium bromide, photographed, and blotted onto a Hybond-N nylon membrane (Amersham) with an LKB vacuum blotter. Membranes were UV cross-linked with a Stratalinker 1800 (Stratagene). The 365-bp rat CD44 cDNA fragment generated by RT-PCR from FBR cells was gel purified and labelled by randomly primed synthesis with Klenow polymerase using a commercial kit (BCL). Hybridization and stringency washes were performed as previously described (70).

For Western blotting, cells were washed thrice in cold phosphate-buffered saline (PBS) and lysed in sodium dodecyl sulfate (SDS) sample buffer (20% glycerol, 2% SDS, 100 mM Tris [pH 6.8], 5% β-mercaptoethanol) containing protease inhibitors, and protein concentrations were measured with a commercial reagent (Bio-Rad). Aliquots of 20 μg of protein were electrophoresed on an SDS–7.5% polyacrylamide gel as described elsewhere (70) and blotted onto polyvinylidene difluoride membranes (Immobilon P; Millipore) with a Transblot wet blotting apparatus (Bio-Rad). Immunoblots were blocked in PBS containing 0.1% Tween 20 and 5% skim milk (Marvel) and probed simultaneously or separately with anti-CD44 MAb 5G8 and antivinculin or antitalin MAbs according to a protocol supplied with the Enhanced Chemiluminescence Western Blotting System (Amersham). Blots were then visualized by exposure to Kodak X-Omat film for various times. Quantitation of autoradiographs by densitometry was performed using a Quantity One one-dimensional analysis program (PDI Inc.) on an image analysis workstation (Molecular Dynamics). For Western blotting of c-*jun*, v-*fos*, and TAM-67, a whole-cell extract was prepared as described previously (50), with samples mixed with an equal volume of 2× SDS sample buffer and processed as described above. Protocols for enhanced chemiluminescence detection using anti-c-*jun* AB-1 and anti-pan-*fos* were as suggested by the manufacturers (respectively, Oncogene Science and Santa Cruz Biotechnology).

Immunofluorescence. For immunofluorescence cells were seeded on four- or eight-well chamber slides (Costar) at approximately 50% confluence and grown for 24 to 48 h prior to treatment or processing. Cells were washed twice with cold PBS and fixed in acetone at −20°C for 10 min. Fixation under the same conditions with methanol or ethanol gave essentially identical results. Blocking of nonspecific antibody binding was performed with blocking buffer (PBS containing 0.1% Tween 20 and 5% skim milk [Marvel]) for 30 min at room temperature. For actin labelling with TRIC-phalloidin, slides were incubated again at room temperature in the above-described buffer containing 0.5 μg of TRIC-phalloidin (Sigma) per ml for 30 min and washed three times at room temperature in blocking buffer alone before coverslip mounting (Vectashield; Vector Laboratories). For indirect immunofluorescence of CD44 alone or in combination with TRIC-phalloidin staining, blocked slides were incubated for 1 h at room temperature in blocking buffer containing a 1/100 dilution of anti-CD44 MAb OX49 or Hermes-3 (for human CD44-GFP fusion) and washed thrice in blocking buffer before incubation for 45 min at room temperature in fresh blocking buffer containing a 1/50 dilution of FITC- or TRIC-labelled anti-mouse IgG (Sigma) alone (for single labelling) or in combination with 0.5 μg of TRIC-labelled phalloidin or FITC-labelled anti-rabbit IgG (Sigma) per ml for double labelling, before washing in blocking buffer and mounting as before. All slides were viewed

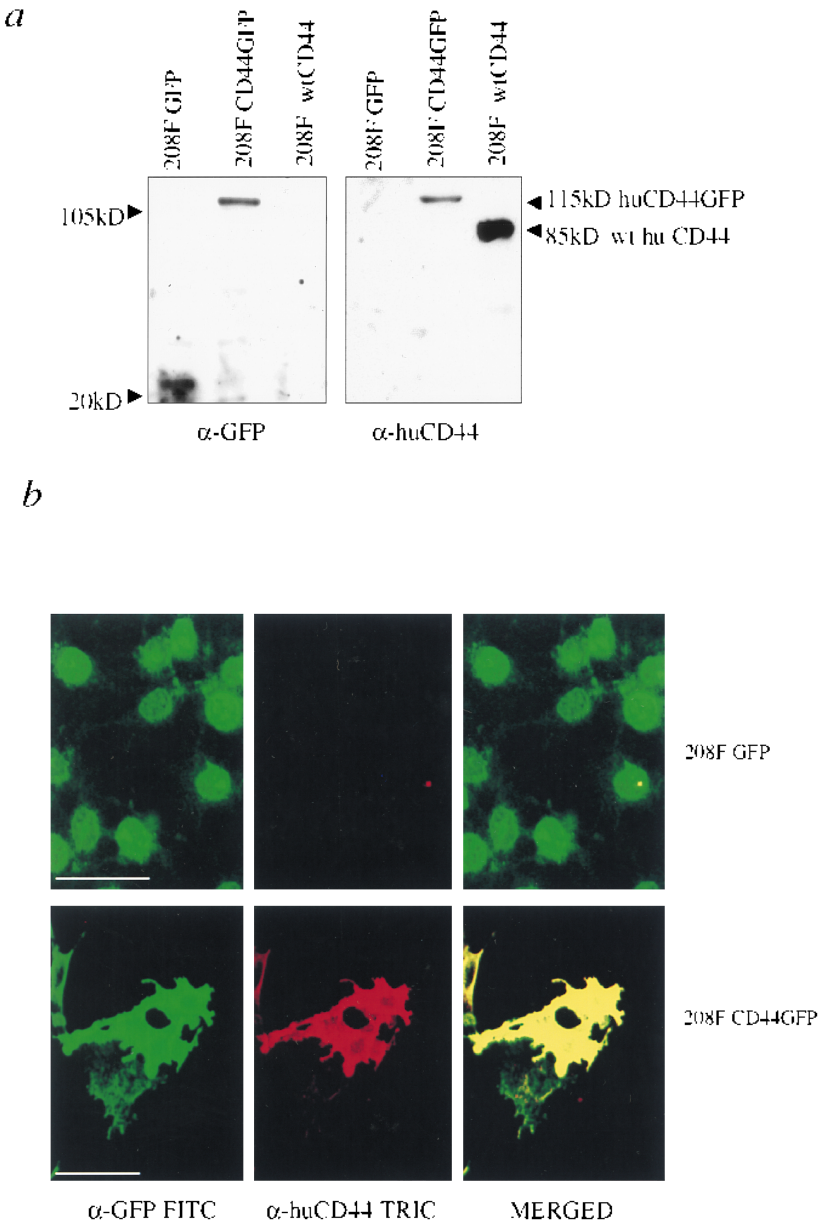

FIG. 5. CD44s-GFP expression and localization in 208F transformed by EGF. (a) Western analysis of GFP, human CD44s-GFP, and human CD44 in 208F stably transfected with GFP (208F GFP), human CD44-GFP fusion (208F CD44GFP), or human CD44 (208F wtCD44). Duplicate immunoblots were probed with GFP-specific antiserum (α-GFP) or human CD44-specific antiserum (α-huCD44). The two molecular size markers shown were from Life Technologies. (b) Coimmunolocalization of human CD44 and GFP in 208F stably transfected with CD44-GFP fusion. Double labelling of 208F stably transfected with GFP or human CD44-GFP fusion (i) with rabbit polyclonal antisera to GFP followed by FITC-labelled anti-rabbit secondary antibody or (ii) with an anti-human CD44-specific mouse MAb (Hermes-3) followed by TRIC-labelled anti-mouse secondary antibody (α-huCD44 TRIC) is shown. Confocal images of red and green channels and a merged image of both channels are shown. Note that colocalization of red and green signals occurs only in CD44-GFP-transfected 208F. Unfused GFP localization is predominantly cytosolic and nuclear, while CD44s-GFP covers the cell membrane. Note also that under these conditions there is overlap between intrinsic GFP fluorescence and fluorescence of the FITC-labelled secondary antibody. (c) Localization of transfected CD44-GFP at pseudopodic extensions after transformation of 208F with EGF. Images of 208F transiently transfected with GFP (208F GFP) or CD44s-GFP (208F CD44GFP) expression constructs in growing cultures (C) or after treatment for 48 h with 40 ng of EGF per ml (+EGF) are shown. Cells were imaged either directly on 9-cm-diameter dishes plastic dishes or on glass chamber slides after fixation with methanol (bottom). Note that GFP under both conditions remains primarily cytosolic after treatment with EGF, with no preferential localization at pseudopodial tips, while significant amounts of CD44s-GFP are associated with these structures (arrowheads). Bars, 25 μm.

on a Bio-Rad MRC 600 confocal illumination unit attached to a Nikon Diaphot inverted microscope with various magnifications. For GFP fluorescence, images either of live cells in 9-cm-diameter dishes or of cells cultured on glass chamber slides after brief washing in cold PBS and fixation for 5 min in ice-cold methanol and coverslip mounting were taken as described above. Fluoresence images were obtained with a conventional FITC exitation setting on the laser confocal microscope as described above and processed as tagged-image file format (TIFF) images.

EGF transformation of 208F. The morphological transformation by EGF was performed essentially as described previously (63). The concentration of growth factor (40 ng/ml) has been shown previously to be required for efficient anchorage-independent growth (41). After 24 to 48 h cells were washed twice in cold PBS and processed for immunofluoresence or Western blotting.

Antisense oligonucleotide inhibition. The phosphorothioate antisense c-*jun* and c-*fos* oligonucleotides used have been described before and specifically downregulate c-*jun* and c-*fos*: jun-AS, 5′-TGC AGT CAT AGA AC-3′; jun-C,

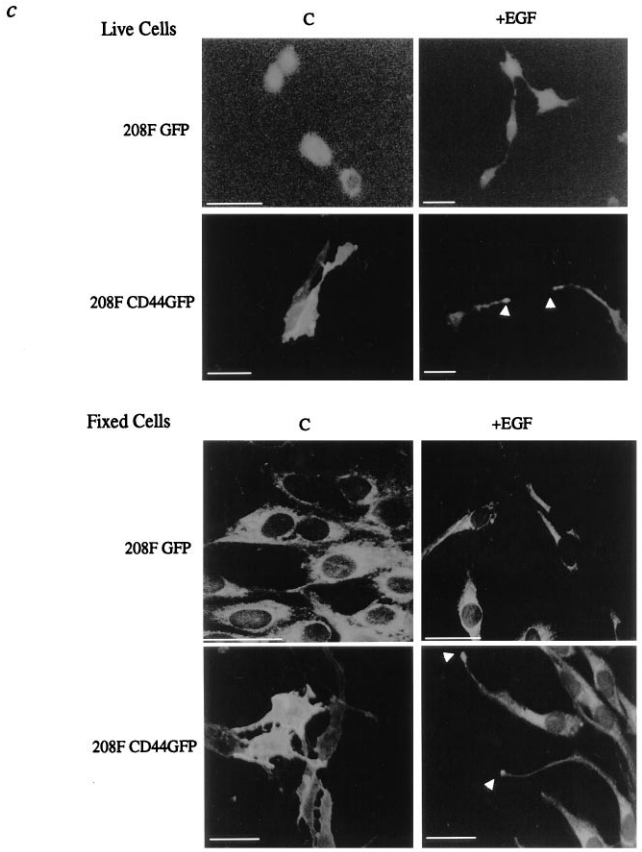

FIG. 5—*Continued.*

5′-GTC CCT ATA CGA AC-3′ (71); SOF (anti-c-*fos*), 5′-GAA GCC CGA GAA CAT CAT-3′; and FOS (sense control), 5′-ATG AGT TTC TCG GGC TTG-3′ (52).

To demonstrate which anti-CD44 oligonucleotides significantly downregulated CD44 expression, underivatized standard oligonucleotides were synthesized complementary to various sequences at the 5′ end of CD44 mRNA (25) and tested for their ability to downregulate CD44 expressed in the FBR v-*fos* transformant. The effect of two of these oligonucleotides is shown in Fig. 4a. (AS2 corresponds to an oligonucleotide complementary to nucleotides 104 to 127 of the rat CD44 sequence of Gunthert et al. [25].) One oligonucleotide (AS1) in particular was effective and reproducible in significantly reducing the level of CD44 detectable by Western blotting after a 24- to 48-h incubation. Phosphorothioate oligonucleotides were synthesized on an ABI 392 DNA synthesizer, deprotected overnight in ammonia at 55°C, and purified by ethanol precipitation. The size and purity of oligonucleotides were demonstrated by denaturing electrophoresis on a 20% polyacrylamide gel (70). Sense or antisense CD44 oligonucleotides used correspond to nucleotides 58 to 74 of the rat CD44 sequence of (25): AS, 5′-GAA AAG GGT CGC GGG GG-3′; S, 5′-CCC CCG CGA CCC TTT TC-3′.

Two methods of oligonucleotide pretreatment were performed. For Western analysis, subconfluent cultures maintained in DMEM containing 10% FCS were washed twice in serum-free DMEM before the addition of DMEM containing 0.5% FCS and 1 μM oligonucleotide. Cells were incubated in this medium for 8 h, washed once with serum-free DMEM before the addition of DMEM containing 0.5% FCS and 40 ng of EGF per ml, and incubated for a further 24 h. For double immunofluoresence the same protocol was followed, except with four modifications designed to more potently suppress CD44 expression. First, 10 μM oligonucleotide was used. Second, pretreatment with oligonucleotide was for 24 rather than 8 h. Third, the medium containing EGF also contained 10 μM fresh oligonucleotide. Fourth, incubation in this medium was extended to 48 h.

In vitro invasion assay. An inverse invasion assay in serum-free conditions was performed and quantitated as previously described (30), using growth factor-depleted Matrigel (Collaborative Research)-coated polycarbonate chambers (Transwell 8-μm-pore-size filters; Costar). In this assay cells are first chemoattracted across a 8-μm-pore-size membrane, those which then migrate into Matrigel are visualized, and cell numbers are quantitated in 10-μm confocal optical sections. By phalloidin staining and three-dimensional confocal reconstruction (29a) cells at 20 μm and above in the Matrigel layer have no cellular contact with the filter and are thus considered to be invasive. For addition of EGF to the assay, human recombinant EGF (Life Technologies) at a concentration of 40 ng/ml was added above the Matrigel layer in serum-free DMEM as previously described for addition of platelet-derived growth factor (30). For oligonucleotide inhibition, 20 μM sense or antisense phosphorothioate CD44 or c-*fos* or 10 μM control or antisense c-*jun* oligonucleotide was added above the Matrigel layer in serum-free DMEM in the presence or absence of 40 ng of EGF per ml. For assays of invasion, 208F cells expressing GFP or CD44s-GFPs were fixed in ice-cold methanol and washed twice in PBS and 10-μm confocal sections were taken with an FITC filter setting on the confocal microscope. Control assays of 208F cells not expressing GFP and processed in this manner were also performed to confirm that GFP fluoresence was being viewed. Results were quantitated by counting GFP- expressing cells in each optical section, expressing those at 20 μm and above as a percentage of GFP-expressing cells in all optical sections. Assays were performed twice in triplicate.

RESULTS

AP-1 components c-*jun* and c-*fos* are required for in vitro invasion. To measure invasion, we used a quantitative in vitro invasion assay which determines the ability of cells to migrate across a membrane and then into a thick layer of the reconstituted ECM, reduced-growth-factor Matrigel (30). In this assay, v-*fos* transformants are constitutively invasive (growth factor independent) while parental 208F fibroblasts are conditionally invasive, dependent upon growth factors. Both cell types are equivalent in their ability to chemotactically migrate across the 8-μm-pore-size membrane (30).

To demonstrate that AP-1 is necessary for in vitro invasion, we used antisense oligonucleotides known to inhibit the synthesis of c-*fos* and c-*jun*. 208F invasion is dependent upon EGF and inhibited by addition of either antisense c-*jun* or c-*fos* oligonucleotide but not by sense c-*jun* or c-*fos* oligonucleotide (Fig. 1a and b). Growth factor-independent invasion of FBR cells is significantly inhibited by antisense c-*jun* but not antisense c-*fos* oligonucleotide (Fig. 1c and d). The c-*fos* antisense oligonucleotide does not inhibit FBR cell invasion, since c-*fos* is not expressed in FBR cells (26a) and the c-*fos* antisense sequence is not present in the viral genome (84).

Dominant negative c-*jun* (TAM-67) inhibits v-*fos*-transformed fibroblast invasion. To further test the role of AP-1 in FBR invasion, we generated FBR transformants stably expressing a deletion mutant of c-*jun* (TAM-67) shown previously to act as a dominant negative inhibitor of AP-1-mediated transformation (14, 64). G418^r FBR subclones expressing TAM-67 (FBR-TAM67) as well as G418^r non-TAM-67-expressing controls (FBR-C) (Fig. 2a) were isolated. The majority of FBR-TAM67 clones have a flat revertant morphology and increased actin stress fibers by TRIC-phalloidin staining (Fig. 2b). The levels of pp75$^{v\text{-}fos}$ are similar in both FBR-TAM67 and FBR-C, excluding deletion of v-*fos* as the reason for the revertant phenotype (Fig. 2a). In the in vitro invasion assay FBR-TAM67 cells are noninvasive in comparison to parental FBR or FBR-C cells (Fig. 2c), indicating that functional AP-1 activity is required for in vitro invasiveness of FBR cells. Immunostaining of FBR-TAM67 for CD44 reveals that it is primarily concentrated at peripheral membrane ruffles and cell surface microvillus processes (Fig. 2b, FBR-TAM67, arrowheads), a distribution similar to that observed in 208F fibroblasts (see Fig. 4a) but distinct from the polarized distribution in FBR and FBR-C (Fig. 2b, FBR-C; see Fig. 4b).

CD44s is upregulated in cells transformed by *fos* or EGF. CD44s has been implicated in both cell motility (79) and invasive growth of tumors (26). The finding that increased expression of CD44 in *ras*-transformed cells is directed by AP-1 (32) suggested that its expression would be increased in Fos-transformed cells. Northern and Western analyses of 208F; two v-*fos* transformants, FBR and FBJ cells; and one c-*fos* trans-

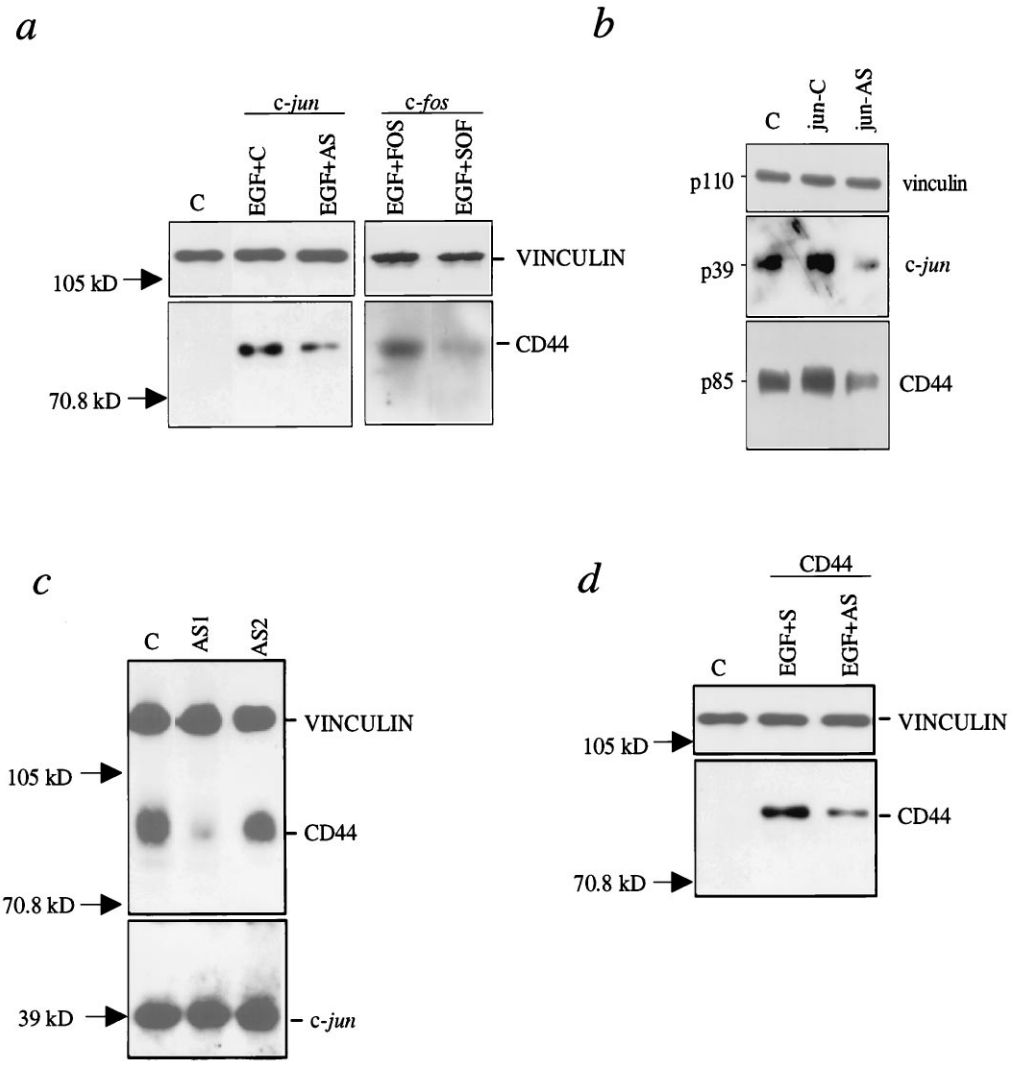

FIG. 6. Antisense-mediated downregulation. (a) Anti-c-*jun* and -c-*fos* oligonucleotides suppress induction of CD44 expression by EGF. Western analysis of CD44 levels in 208F (C) or 208F treated with EGF and control c-*jun* (EGF+C), sense c-*fos* (EGF+FOS), or antisense c-*jun* (EGF+AS) or c-*fos* (EGF+SOF) phosphorothioate oligonucleotide is shown. Immunolots were reprobed with antivinculin MAb to control for loading and transfer. (b) Anti-c-*jun* oligonucleotide downregulates $p39^{c\text{-}jun}$. Immunoblots of FBR cells (C) or FBR cells treated for 24 h with control (jun-C) or anti-c-*jun* (jun-AS) oligonucleotide are shown. Blots were probed with anti-c-*jun*-specific antibody (AB-1) and then reprobed with anti-CD44 and antivinculin MAbs. Densitometric scanning of appropriate autoradiographic exposures reveals an 80% reduction in $p39^{c\text{-}jun}$ and a 50 to 60% reduction in CD44 levels after treatment with anti-c-*jun* oligonucleotide. (c) Anti-CD44 oligonucleotide downregulates p85 CD44. Immunoblots of FBR cells (C) or FBR cells treated for 48 h with two different anti-CD44 oligonucleotides (AS1 and AS2) are shown. Treatment with anti-CD44 oligonucleotide AS1 results in a 70 to 80% reduction in p85 CD44 levels after densitometric scanning of appropriate autoradiographic exposures. Duplicate immunoblots were simultaneously probed with anti-CD44 MAb 5G8 and antivinculin MAb or with anti-c-*jun* antibody to control for loading and possible nonspecific effects of antisense oligonucleotides on protein synthesis, respectively. (d) Anti-CD44 oligonucleotide AS1 suppresses induction of CD44 by EGF. Western analysis of CD44 levels in 208F (C) or 208F treated with EGF and sense (EGF+S) or antisense (EGF+AS) CD44 oligonucleotide is shown. Immunolots were reprobed with antivinculin MAb to control for loading and transfer.

formant, MMV, reveal that CD44 is upregulated in all three *fos* transformants compared to 208Fs. The increase in CD44 expression occurs in growing or growth-arrested FBR, FBJ, and MMV transformants (Fig. 3a and b). This indicates that CD44 upregulation is a consequence of *fos* transformation, not of serum-dependent growth. *ras* transformation results in the appearance of CD44 splice variants as well as increased expression of CD44s mRNAs (32). Three mRNA transcripts with approximate sizes of 4.3, 2.9, and 2.0 kb are detected as previously described in rat cells expressing only CD44s (25, 37). Semiquantitative RT-PCR of 208F and FBR total cell RNA with primers spanning the region of differential splicing (25) indicates that CD44s is the major species upregulated by v-*fos* (Fig. 3c). No RT-PCR products consistent with alternative splicing were detected in 208F or FBR cells in assays where splice variants were detectable by RT-PCR of RNA isolated from rat cells known to express CD44 splice variants (data not shown).

208F can be reversibly induced to adopt the transformed cell morphology and anchorage-independent growth characteristics of v-*fos* transformants by treatment with growth factors (41, 63). EGF-induced transformation of 208F also induces a

four- to sixfold increase in the levels of CD44s mRNA and protein (Fig. 3c and d). No splice variants were detected in EGF-transformed cells at the level of RT-PCR followed by Southern analysis of the PCR products (data not shown). However, it is formally possible that splice variants are expressed in 208F and the transformed cells at levels not detected by these assays.

CD44s is localized at pseudopodial extensions after EGF transformation of 208F and in v-*fos* transformants. To determine if morphological transformation altered the cellular location of CD44s, we compared the distribution of CD44s in FBR, FBJ, and 208F cells in the presence or absence of EGF. 208F cells have a flat morphology with abundant actin stress fibers typical of many immortalized fibroblast lines (63). Immunoreactive CD44s is concentrated at plasma membrane microvilli and peripheral membrane ruffles (Fig. 4a, arrowheads), similar to the localization in normal fibroblasts reported previously by others (82). Transformation of 208F by FBR virus, FBJ virus (30, 56), or EGF (63) induces an elongated, bipolar morphology with extended pseudopodia, structures thought to be important for cell invasion (20, 24). Immunostaining reveals a marked concentration of CD44s at the tips of these extended processes in EGF-transformed (Fig. 4a, +EGF, arrowheads) or v-*fos*-transformed (Fig. 4b) 208F fibroblasts. To exclude the possibility that this apparent polarized concentration of CD44s in the transformed cells was a result of immunofluoresence artifacts, we constructed a fusion of human CD44 with the cell-autonomous fluorescent tag *A. victoria* GFP at the cytoplasmic C terminus of CD44s (CD44s-GFP). Selective recognition using antibodies to the transfected human CD44s (59) or to GFP indicates that a correctly sized and membrane-localized CD44s-GFP fusion protein is expressed in stably transfected 208F cells (Fig. 5a and b). In 208F transiently expressing either CD44s-GFP or GFP only, CD44s-GFP is concentrated at the ends of pseudopodial cell extensions in both live (Fig. 5c, top panel) and fixed (Fig. 5c, bottom panel) EGF-transformed cells.

Induction of CD44 expression by EGF requires AP-1 components c-*jun* and c-*fos* but is not required for morphological transformation. EGF has been shown to upregulate the expression of an AP-1-responsive gene, that for stromelysin, through a requirement for c-*jun* and c-*fos* expression (52). We tested whether induction of CD44 by EGF also depends upon AP-1 components by using the antisense c-*jun* and c-*fos* oligonucleotides, which inhibit invasion. Pretreatment of 208F with antisense c-*jun* or c-*fos* oligonucleotide significantly inhibits the EGF-induction of CD44 in comparison to control oligonucleotides (Fig. 6a). The effectiveness of these oligonucleotides in downregulating expression of c-*jun* (71) and c-*fos* (52) has been shown previously and is shown for c-*jun* in Fig. 6b. Quantitation of autoradiographs of Western blots of extracts from antisense c-*jun* oligonucleotide-treated FBR cells reveals an 80% reduction in c-*jun* and a parallel 50 to 60% reduction of CD44s in comparison to controls (Fig. 6b).

The intracellular C-terminal tail domain of CD44s has been shown previously to interact with cytoskeletal protein ankyrin (9, 10, 48) and with members of the ERM family (82), the latter of which have also been shown to influence cell shape (77). The prototype of this family, ezrin, has also been shown to be upregulated by v-*fos* transformation (40). CD44s upregulation, altered cellular localization, and purported interaction with ezrin suggested that it is involved in morphological transformation by EGF or *v-fos*. We designed several antisense oligonucleotides directed against the 5′ end of CD44 mRNA, and found one (AS1) particularly effective in decreasing the expression of CD44 in FBR cells and in inhibiting induction of

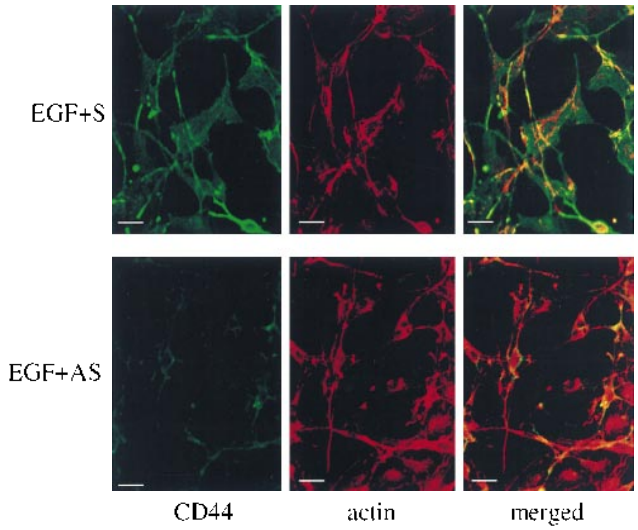

FIG. 7. Morphological change induced by EGF occurs in the absence of CD44 immunostaining. Double labelling of EGF-transformed 208F pretreated for 24 h with sense (EGF+S) or antisense (EGF+AS) CD44 oligonucleotide followed by EGF treatment for 48 h with TRIC-phalloidin for actin (red) and CD44 (green) is shown. Single images of CD44 and TRIC-phalloidin (actin)-labelled cells and a merged image of the two are shown. Pretreatment of 208F with either sense or antisense CD44 oligonucleotide has no effect on the morphological transformation induced by EGF, as indicated by cortical actin staining (red) and elongated pseudopodia. The majority of cells (>85% [data not shown]) undergo this shape change in response to EGF after pretreatment with either sense or antisense oligonucleotide. Note the paucity of green (CD44) immunostaining after treatment with antisense but not sense CD44 oligonucleotide, indicating that this EGF-induced shape change occurs in the absence of detectable CD44 expression. Bars, 25 μm.

CD44 expression in 208F cells by EGF (Fig. 6c and d). However, AS1 did not suppress EGF-induced morphological transformation of 208F even at a relatively high (10 μM) concentration of oligonucleotides, which resulted in an almost complete ablation of CD44s immunostaining (Fig. 7). Similarly, downregulation of CD44s by AS1 has no effect on the elongated bipolar morphology of FBR (data not shown).

CD44s is required for invasion. CD44s expression can be inhibited by antisense oligonucleotide AS1. When added to the inverse invasion assay, AS1 significantly inhibits invasion of both 208F fibroblasts in response to EGF and FBR cells in comparison to sense oligonucleotide (Fig. 8a to d) or a scrambled-sequence oligonucleotide (data not shown). Another antisense CD44 oligonucleotide, AS2, which does not inhibit CD44s expression significantly (Fig. 6c), has no effect on invasion either of 208F fibroblasts in response to EGF or of FBR cells (data not shown).

To exclude the possibility that downregulation of CD44s by AS1 primarily inhibits chemotaxis of cells across the 8-μm-pore-size membrane prior to contact with Matrigel, we examined the migration of cells across the filter in response to EGF in the presence of AS1. No inhibition of chemotaxis was observed in the presence of AS1 compared to that with sense oligonucleotides, indicating that increased CD44s expression is required for migration of the cells into the Matrigel (Fig. 8e and f). To determine whether increased CD44s expression could stimulate the invasion of 208F fibroblasts in the absence of EGF, we introduced CD44s-GFP and GFP cDNA expression vectors separately into 208F cells and tested their ability in invade. Both CD44s-GFP-expressing 208F and GFP-expressing 208F cells require EGF for invasion (Fig. 9). The CD44s-GFP expression vector lacks the AS1 sequence (59), and

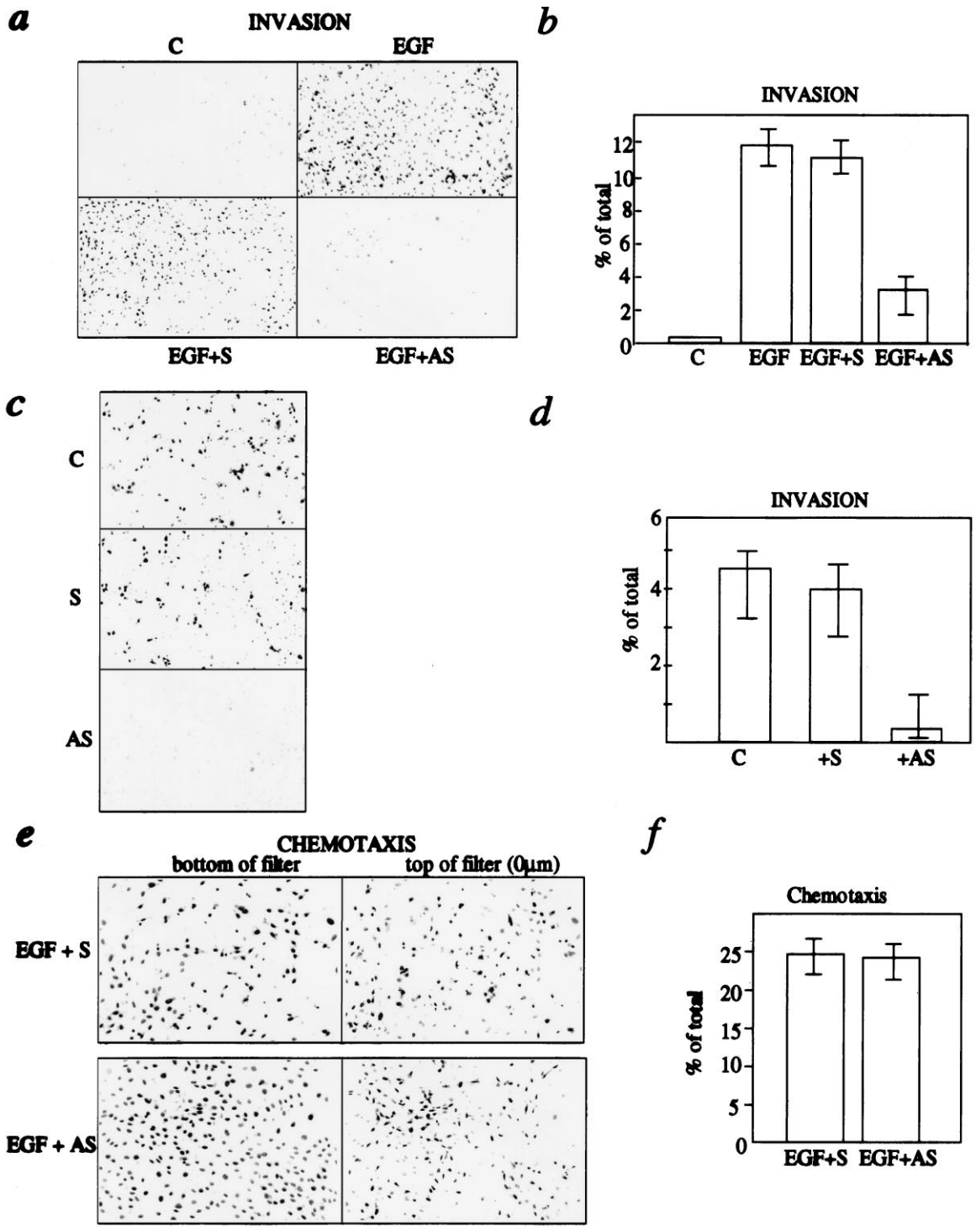

FIG. 8. Anti-CD44 oligonucleotide inhibits v-*fos*- or EGF-induced ECM invasion. (a) Confocal images of propidium iodide-stained cell nuclei at 20 μm in Matrigel of 208F in the absence (C) or presence of EGF alone or in the presence of sense (EGF+S) or antisense (EGF+AS) CD44 phosphorothioate oligonucleotide. (b) Quantitative analysis of invasion. Invasion assay results were quantitated as in Fig. 1b with a Bio-Rad program (Comos) and represent the average from at least four separate assays in two experiments. (c) v-*fos* FBR invasion. Confocal images of propidium iodide-stained cell nuclei at 20 μm in Matrigel of v-*fos* FBR cells in the absence (C) or presence of sense (S) or antisense (AS) CD44 phosphorothioate oligonucleotide are shown. (d) Quantitative analysis of FBR cell invasion. Invasion assay results were quantitated as in Fig. 1b. (e) Chemotaxis of 208F in response to EGF in addition to sense or antisense CD44 oligonucleotides. Confocal images are of cells on the bottom of the filter and those chemoattracted across the filter (0μm). (f) Quantitative analysis of chemotaxis. Quantitation of chemotaxis in this invasion assay has been described previously (30) and represents the percentage of positive pixels in all of the confocal sections above the filter bottom, where 100% is the positive pixels in all confocal sections. Quantitation represents the average from at least four separate assays in two experiments.

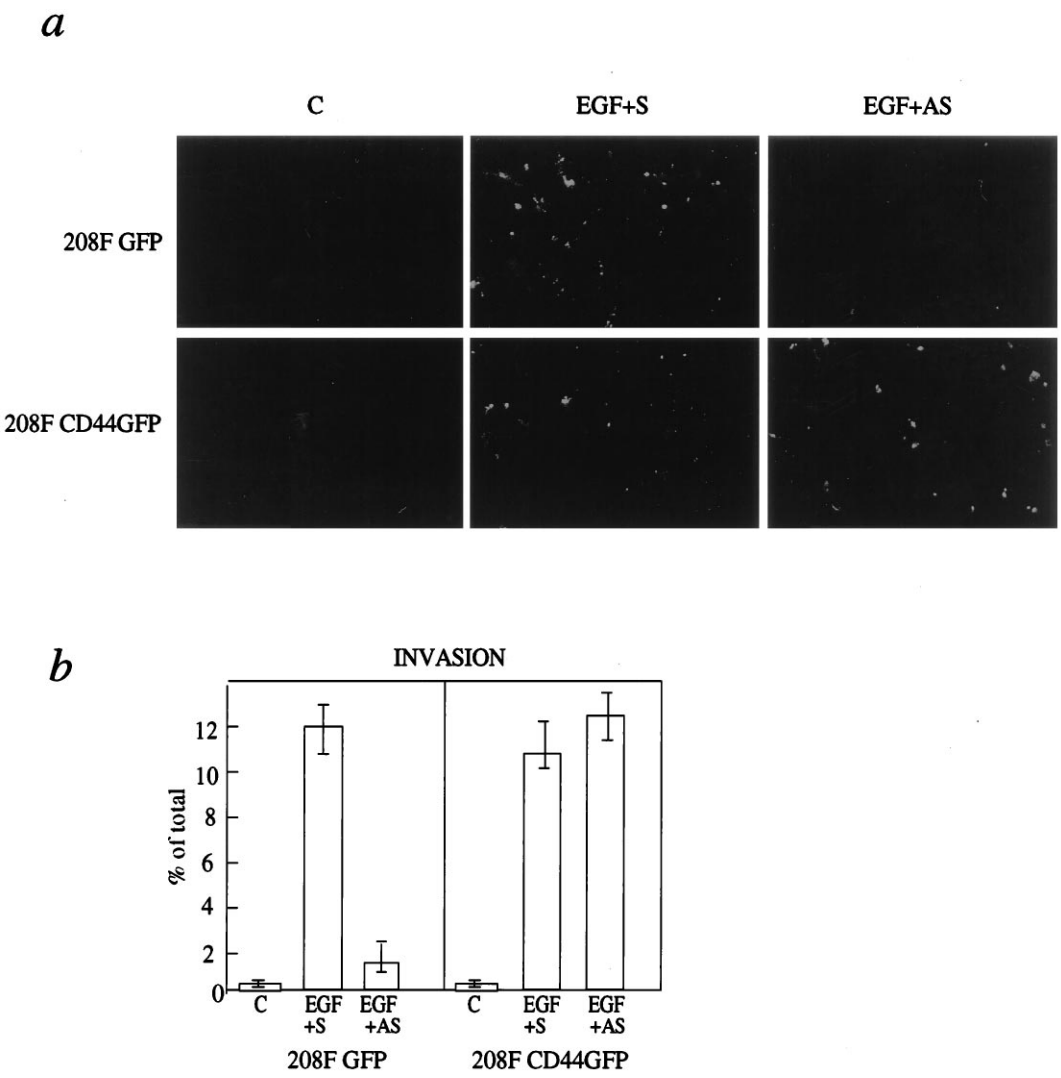

FIG. 9. Invasion of 208F expressing GFP or CD44-GFP. (a) Representative confocal images of GFP fluorescence at 20 μm in Matrigel of 208F expressing GFP (208F GFP) or CD44-GFP fusion (208F CD44GFP) in the absence (C) or presence of EGF with sense (EGF+S) or antisense (EGF+AS) CD44 phosphorothioate oligonucleotide are shown. Note that GFP fluorescence at 20 μm is absent in invasion assays lacking EGF for both 208F GFP and 208F CD44s-GFP. Cell bodies with GFP fluorescence are detected in the presence of EGF with anti-CD44 oligonucleotide only for CD44s-GFP chimera-expressing 208F. (b) Quantitation of invasion. Invasion assay results of CD44s-GFP- and GFP-expressing cells were quantitated as described in Materials and Methods.

CD44s-GFP-expressing 208F but not GFP-expressing 208F cells invade in the presence of AS1 and EGF. This demonstrates that CD44s-GFP expression complements AS1-mediated inhibition of invasion (Fig. 9, EGF+AS), further substantiating the idea that CD44s expression is required for invasion and demonstrating that AS1 does not inhibit invasion by a nonspecific mechanism.

DISCUSSION

Although AP-1 can function as a critical regulator of cell cycle progression (33, 43, 60, 65), transformation by v- or c-*fos* induces the expression of a number of genes encoding proteins with no clear role in proliferation but with demonstrated involvement in cytoskeletal rearrangement, cell motility, or proteolysis of ECM (30, 40, 55). Using a quantitative in vitro invasion assay, we have shown that v-*fos* transformants can be distinguished from 208F cells by their ability to invade into reduced-growth-factor Matrigel (30) in the absence of added growth factors. In contrast, 208F invasion is dependent upon the addition of EGF or platelet-derived growth factor (30). Our data demonstrate that FBR *v-fos*- and EGF-induced in vitro invasions require functional components of the AP-1 transcription factor and the expression of an AP-1-regulated gene, the CD44 gene. On the basis of these results we propose that prolonged activation of AP-1 by growth factors, oncogenes which function upstream of AP-1, or *v-fos* results in increased expression of AP-1-dependent genes which mediate in vitro invasion.

fos-transformed cells phenotypically mimic cells transformed by *ras*, *raf*, and *sis* in many in vitro assays of cell transformation such as anchorage-independent growth, loss of contact inhibition, adoption of a spindle-like morphology, and ECM invasion. In Fos and other oncogene transformants there is a gross cytoskeletal reorganization which results in a diminution of actin stress fibers and focal contacts (30, 56). However, unlike the other oncogene-transformed fibroblasts, Fos transformants require the presence of serum-derived mitogens for prolifera-

tion and growth arrest in reduced serum (27, 30, 40). Moreover, c-*fos*- and c-*jun*-containing AP-1 complexes are crucially required for the transforming ability of a variety of other oncogenes which function in signalling cascades upstream of c-*fos* (39, 47, 64, 76). Recent data from an inducible system indicate that c-*fos* is also capable of morphologically transforming fibroblasts independent of their cycling status (55). Both sets of data are consistent with the idea that c-*fos*- and c-*jun*-containing AP-1 complexes may modulate the morphological changes characteristic of oncogene transformation.

Consistent with the data presented here, recent studies of mice rendered c-*fos* null through gene targeting further suggest that c-*fos* functions in both ECM remodelling and malignant conversion. Thus, c-*fos*-null mice develop bone abnormalities, including osteopetrosis, suggesting that a c-*fos*-induced program of gene expression is required for matrix remodelling during bone development (23). Similarly, induction of skin tumors in c-*fos*-null mice exposed to chemical carcinogens or activated *ras* oncogenes has shown also that c-*fos* is necessary for conversion of premalignant papillomas to malignant skin carcinomas and for induction of AP-1-regulated matrix proteases (69).

We have demonstrated that an AP-1-directed increase in CD44s expression is required for in vitro invasion into Matrigel. CD44s is a cell surface transmembrane proteoglycan and appears to mediate a diverse range of functions in different cell types (28, 73). CD44s has been shown to function in both cell-cell and cell-ECM interactions through binding to hyaluronan, fibronectin, collagen, and osteopontin (5, 36, 75, 85). Interestingly, CD44s expression in fibroblasts and the hyaluronan content of ECM are elevated during normal fibroblast invasiveness in wound repair (49, 54), consistent with a link between CD44 induction and invasion.

As well as CD44s, a number of structural variants generated through alternative splicing (28) which may increase the aggressiveness of human tumors (51, 58) have been described and have been claimed to increase metastatic tumor formation in a rat model system (25). A widely expressed splice variant of CD44 is involved in invasion in vitro of CD44-expressing glioblastoma cell lines (53). However, whether expression and invasive function of CD44 in glioblastoma or other tumor-derived cell lines are results of deregulation of AP-1 or of deregulated signalling due to other genetic lesions has yet to be established. Our results indicate that AP-1-directed increased expression of CD44s, which is expressed in a greater variety of tissues than splice variants of CD44 (28, 73), plays an important role in fibroblast invasion.

Our results indicate a recruitment of CD44s to pseudopodial extensions of EGF- or v-*fos*-transformed cells. Motile pseudopods are thought to be involved in the movement of fibroblasts through three-dimensional matrices (80) and may mediate tumor cell migration on components of ECM (24). Clustering of CD44 at such sites may therefore serve to enhance local adhesion and degradation of hyaluronan or other ECM components and hence promote cell migration. Clustering of CD44 has been shown to markedly increase its affinity for hyaluronate (45, 83), while interaction of CD44s via its cytoplasmic domain with components of the underlying cytoskeleton has also been shown to modulate hyaluronan binding (48). Cytoskeletal linking proteins of the ERM family are potential candidates for linking CD44s with the actin-based cytoskeleton (82). Interestingly, a member of the ERM family, ezrin, has also been shown to be upregulated in 208F transformed by v-*fos* (40) or EGF and to colocalize with CD44s at the tips of pseudopods (43a).

In conclusion, the results presented here demonstrate that AP-1 is required for fibroblast invasion and that increased expression of at least one AP-1-regulated gene, CD44, is required for this process. These results support the proposal that Fos transforms fibroblasts by constitutively activating an AP-1-regulated multigenic invasion program. A similar analysis of the role of other v-*fos*/AP-1 target genes in cells transformed by oncogenes which function upstream of AP-1 will help to determine the general validity of this proposal.

ACKNOWLEDGMENTS

We thank Jonathan Sleeman and Eugene Butcher for generously providing anti-rat and anti-human CD44 antibodies, respectively. We are also particularly grateful to Peter McHardy for guidance with the MRC 600 confocal microscope. We also thank Clare Isacke and Michael Birrer, respectively, for the pSRαneo and pSRαneoCD44 and the pCMV TAM-67 expression constructs; to Paul Mangeat and Dave Gillespie for useful discussion; and to John Wyke for critical reading of the manuscript. R.F.L. is grateful to Ian Pickford for continued support throughout this work.

This work was carried out with support from the Cancer Research Campaign and the Scottish Home and Health Department. K.D.K. is supported by a scholarship in cell biology from the Greek State Scholarship Foundation. R.F.L. is supported by a grant from the Medical Research Council.

REFERENCES

1. **Acari, P., R. Martinelli, and F. Salvatore.** 1984. The complete nucleotide sequence of a full length cDNA for human liver glyceraldehyde-3-phosphate dehydrogenase: evidence for multiple mRNA species. Nucleic Acids Res. **12:**9179–9189.
2. **Agren, M. S., C. J. Taplin, J. F. Woessner, W. H. Eaglstein, and P. M. Mertz.** 1992. Collagenase in wound healing: effect of wound age and type. J. Invest. Dermatol. **99:**709–714.
3. **Angel, P., M. Imagawa, R. Chiu, B. Stein, R. J. Imbra, H. J. Rahmsdorf, C. Jonat, P. Herrlich, and M. Karin.** 1987. Phorbol ester-inducible genes contain a common *cis* element recognized by a TPA-modulated *trans*-acting factor. Cell **49:**729–735.
4. **Angel, P., K. Hattori, T. Smeal, and M. Karin.** 1988. The *jun* proto-oncogene is positively autoregulated by its product, *jun*/AP-1. Cell **55:**875–885.
5. **Aruffo, A., I. Stamenkovic, M. Melnick, C. B. Underhill, and B. Seed.** 1990. CD44 is the principal cell surface receptor for hyaluronate. Cell **61:**1303–1313.
6. **Bartolazzi, A., R. Peach, A. Aruffo, and I. Stamenkovic.** 1994. Interaction between CD44 and hyaluronate is directly implicated in the regulation of tumour development. J. Exp. Med. **180:**53–66.
7. **Bennett, K. L., D. G. Jackson, J. C. Simon, E. Tanczos, R. Peach, B. Modrell, I. Stamencovich, G. Plowman, and A. Aruffo.** 1995. CD44 isoforms containing exon v3 are responsible for the presentation of heparin-binding growth factor. J. Cell Biol. **128:**687–698.
8. **Birch, M., S. Mitchell, and I. R. Hart.** 1991. Isolation and characterization of melanoma cell variants expressing high and low levels of CD44. Cancer Res. **51:**6660–6667.
9. **Bourguignon, L. Y. W., V. B. Lokeshwar, J. He, X. Chen, and G. J. Bourguignon.** 1992. A CD44-like endothelial cell transmembrane glycoprotein (GP116) interacts with extracellular matrix and ankyrin. Mol. Cell. Biol. **12:**4464–4471.
10. **Bourguignon, L. Y. W., V. B. Lokeshwar, X. Chen, and W. G. L. Kerrick.** 1993. Hyaluronic acid-induced lymphocyte signal transduction and HA receptor (GP85/CD44)-cytoskeleton interaction. J. Immunol. **151:**6634–6644.
11. **Brenner, C. A., M. O'Hara, P. Angel, M. Chojkier, and M. Karin.** 1989. Prolonged activation of *jun* and collagenase genes by tumor necrosis factor-α. Nature **337:**661–663.
12. **Brown, P. H., T. K. Chen, and M. J. Birrer.** 1994. Mechanism of action of a dominant-negative c-Jun. Oncogene **9:**791–799.
13. **Brusselbach, S., U. Mohle-Steinlein, Z. Q. Wang, M. Schreiber, F. C. Lucibello, R. Muller, and E. F. Wagner.** 1995. Cell proliferation and cell cycle progression are not impaired in fibroblasts and ES cells lacking c-*fos*. Oncogene **10:**79–86.
14. **Chen, T. K., L. M. Smith, D. K. Gebhardt, M. J. Birrer, and P. H. Brown.** 1996. Activation and inhibition of the AP-1 complex in human breast cancer cells. Mol. Carcinog. **15:**215–226.
15. **Cochran, B. H., J. Zullo, I. M. Verma, and C. D. Stiles.** 1984. Expression of the c-*fos* oncogene and of a *fos*-related gene is stimulated by platelet-derived growth factor. Science **226:**1080–1082.
16. **Cohen, D. R., and T. Curran.** 1988. *fra*-1: a serum-inducible, cellular immediate-early gene that encodes a Fos-related antigen. Mol. Cell. Biol. **8:**2063–2069.

17. **Culty, M., H. A. Nguyen, and C. B. Underhill.** 1992. The hyaluronan receptor (CD44) participates in the uptake and degradation of hyaluronan. J. Cell Biol. **116:**1055–1062.
18. **Curran, T.** 1989. Fos, p. 307–325. *In* E. P. Reddy, A. M. Skalka, and T. Curran (ed.), An oncogene handbook. Elsevier, Amsterdam, The Netherlands.
19. **Faassen, A. E., J. A. Schrager, D. J. Klein, T. D. Oegema, J. R. Couchman, and J. B. McCarthy.** 1992. A cell surface chondroitin sulphate proteoglycan, immunologically related to CD44, is involved in type 1 collagen-mediated melanoma cell motility and invasion. J. Cell Biol. **116:**512–531.
20. **Gailit, J., and R. A. F. Clark.** 1994. Wound repair in the context of extracellular matrix. Curr. Opin. Cell Biol. **6:**717–725.
21. **Girard, M. T., M. Matsubara, C. Kublin, M. J. Tessier, C. Cintron, and M. E. Fini.** 1993. Stromal fibroblasts synthesize collagenase and stromelysin during long-term tissue remodeling. J. Cell Sci. **104:**1001–1011.
22. **Greenberg, M. E., and E. B. Ziff.** 1984. Stimulation of 3T3 cells induces transcription of the c-*fos* proto-oncogene. Nature **311:**433–438.
23. **Grigoriadis, Z., M. Wang, W. Cecchini, R. Hofstetter, R. Felix, A. Fleisch, and E. F. Wagner.** 1994. c-Fos: a key regulator of osteoclast-macrophage lineage determination and bone remodeling. Science **266:**443–448.
24. **Guirguis, R., I. Margulies, G. Taraboletti, E. Schiffmann, and L. Liotta.** 1987. Cytokine-induced pseudopodial protrusion is coupled to tumour cell migration. Nature **329:**261–263.
25. **Gunthert, U., M. Hofmann, W. Rudy, S. Reber, M. Zoller, L. Haussmann, S. Matzku, A. Wenzel, H. Ponta, and P. Herrlich.** 1991. A new variant of glycoprotein CD44 confers metastatic potential to rat carcinoma cells. Cell **65:**13–21.
26. **Guo, Y., J. Ma, J. Wang, X. Che, J. Narula, M. Bigby, M. Wu, and M.-S. Sy.** 1994. Inhibition of human melanoma growth and metastasis *in vivo* by anti-CD44 monoclonal antibody. Cancer Res. **54:**1561–1565.

26a. **Hawker, K. L., L. McGarry, and B. Ozanne.** Unpublished results.

27. **Hawker, K. L., A. Pintzas, R. F. Hennigan, D. A. F. Gillespie, and B. W. Ozanne.** 1993. Transformation by the *fos* or *jun* oncogene does not increase AP-1 DNA-binding activity. J. Virol. **67:**5487–5495.
28. **Haynes, B. F., H.-X. Liao, and K. L. Patton.** 1991. The transmembrane hyaluronate receptor (CD44): multiple functions, multiple forms. Cancer Cells **3:**347–350.
29. **Heim, R., A. B. Cubitt, and R. Y. Tsien.** 1995. Improved green fluoresence. Nature **373:**663–664.

29a. **Hennigan, R. F.** Unpublished observations.

30. **Hennigan, R. F., K. L. Hawker, and B. W. Ozanne.** 1994. Fos-transformation genes associated with invasion. Oncogene **9:**3591–3600.
31. **Hirai, S.-I., R.-P. Rysek, R. Mechta, R. Bravo, and M. Yaniv.** 1991. Characterization of jun D: a new member of the *jun* proto-oncogene family. EMBO J. **8:**1433–1439.
32. **Hofmann, M., W. Rudy, U. Gunthert, S. G. Zimmer, V. Zawadzki, M. Zoller, R. B. Lichtner, P. Herrlich, and H. Ponta.** 1993. A link between *ras* and metastatic behaviour of tumour cells: *ras* induces CD44 promoter activity and leads to low-level expression of metastasis-specific variants of CD44 in CREF cells. Cancer Res. **53:**1516–1521.
33. **Holt, J. T., R. L. Redner, and A. W. Nienhuis.** 1986. Inducible production of c-fos antisense RNA inhibits 3T3 cell proliferation. Proc. Natl. Acad. Sci. USA **83:**4794–4798.
34. **Hu, E., E. Mueller, S. Oliviero, E. Papaioannou, R. Johnson, and B. M. Spiegelman.** 1994. Targeted gene disruption of the c-*fos* gene demonstrates c-*fos*-dependent and -independent pathways for gene expression stimulated by growth factors or oncogenes. EMBO J. **13:**3094–3103.
35. **Isacke, C. M.** 1994. The role of the cytoplasmic domain in regulating CD44 function. J. Cell Sci. **107:**2353–2359.
36. **Jalkanen, S., and M. Jalkanen.** 1992. Lymphocyte CD44 binds the COOH-terminal heparin-binding domain of fibronectin. J. Cell Biol. **116:**817–835.
37. **Jamal, H. H., D. F. Cano-Gauci, R. N. Buick, and J. Filmus.** 1994. Activated *ras* and *src* induce CD44 overexpression in rat intestinal epithelial cells. Oncogene **9:**417–423.
38. **Jamal, S., and E. Ziff.** 1990. Transactivation of c-*fos* and β-actin genes by *raf* as a step in early response to transmembrane signals. Nature **344:**463–466.
39. **Johnson, R., B. Spiegelman, D. Hanahan, and R. Wisdom.** 1996. Cellular transformation and malignancy induced by *ras* require c-*jun*. Mol. Cell. Biol. **16:**4504–4511.
40. **Joos, K. U., and R. Muller.** 1995. Deregulation of genes encoding microfilament-associated proteins during Fos-induced morphological transformation. Oncogene **10:**603–608.
41. **Kaplan, P. L., and B. W. Ozanne.** 1983. Cellular responsiveness to growth factors correlates with a cell's ability to express the transformed phenotype. Cell **33:**931–938.
42. **Kerr, L. D., J. T. Holt, and L. M. Matrisian.** 1988. Growth factors regulate transin gene expression by c-*fos*-dependent and c-*fos*-independent pathways. Science **242:**1424–1427.
43. **Kovary, K., and R. Bravo.** 1991. The Jun and Fos protein families are both required for cell cycle progression in fibroblasts. Mol. Cell. Biol. **11:**4466–4472.

43a. **Lamb, R. F., B. W. Ozanne, and P. Mangeat.** Unpublished observations.

44. **Lee, W., P. Mitchell, and R. Tjian.** 1987. Purified transcription factor AP-1 interacts with TPA-inducible enhancer elements. Cell **49:**741–752.
45. **Lesley, J., Q. He, K. Miyake, A. Hamann, R. Hyman, and P. W. Kincade.** 1992. Requirements for hyaluronic acid binding by CD44: a role for the cytoplasmic domain and activation by antibody. J. Exp. Med. **175:**257–266.
46. **Litz-Jackson, S., A. H. Miller, G. S. Burgess, and H. S. Boswell.** 1992. Dissociation of nuclear events on p21 RAS transformation of FDC-P1 myeloid cells: c-*jun*/AP-1 expression versus c-*myc* transcription. Blood **79:**2404–2414.
47. **Lloyd, A., N. Yanchevak, and B. Wasylyk.** 1991. Transformation suppressor activity of a jun transcription factor lacking its activation domain. Nature **352:**635–638.
48. **Lokeshwar, V. B., N. Fregien, and L. Y. W. Bourguignon.** 1994. Ankyrin-binding domain of CD44 (GP85) is required for the expression of hyaluronic acid-mediated adhesion function. J. Cell Biol. **126:**1099–1109.
49. **Lorenz, H. P., and N. S. Adzick.** 1993. Scarless skin wound repair in the fetus. West. J. Med. **159:**350–355.
50. **Marais, R., J. Wynne, and R. Treisman.** 1993. The SRF accessory protein ELK-1 contains a growth factor-regulated transcriptional activation domain. Cell **73:**381–393.
51. **Mayer, B., K. W. Jauch, U. Gunthert, C. G. Figdor, F. W. Schildberg, I. Funke, and J. P. Johnson.** 1993. De-novo expression of CD44 and survival in gastric cancer. Lancet **342:**1019–1022.
52. **McDonnell, S. E., L. D. Kerr, and L. M. Matrisian.** 1990. Epidermal growth factor stimulation of stromelysin mRNA in rat fibroblasts requires induction of proto-oncogenes c-*fos* and c-*jun* and activation of protein kinase C. Mol. Cell. Biol. **10:**4284–4293.
53. **Merzak, A., S. Koocheckpour, and G. J. Pilkington.** 1994. CD44 mediates human glioma cell adhesion and invasion *in vitro*. Cancer Res. **54:**3988–3992.
54. **Messadi, D. V., and C. N. Bertolami.** 1993. CD44 and hyaluronan expression in human cutaneous scar fibroblasts. Am. J. Pathol. **142:**1041–1049.
55. **Miao, G. G., and T. Curran.** 1994. Cell transformation by c-*fos* requires an extended period of expression and is independent of the cell cycle. Mol. Cell. Biol. **14:**4295–4310.
56. **Miller, A. D., T. Curran, and I. M. Verma.** 1984. c-*fos* protein can induce cellular transformation: a novel mechanism of activation of a cellular oncogene. Cell **35:**51–60.
57. **Miyake, K., C. B. Underhill, J. Lesley, and P. W. Kincade.** 1990. Hyaluronate can function as a cell adhesion molecule and CD44 participates in hyaluronate recognition. J. Exp. Med. **172:**69–75.
58. **Mulder, J. W., P. M. Kruyt, M. Sewnath, J. Oosting, C. A. Seldenrijk, W. F. Weidema, G. J. Offerhaus, and S. T. Pals.** 1994. Colorectal cancer prognosis and expression of exon-v6-containing CD44 proteins. Lancet **344:**1470–1472.
59. **Neame, S., and C. Isacke.** 1993. The cytoplasmic tail of CD44 is required for basolateral localization in epithelial MDCK cells but does not mediate association with the detergent-insoluble cytoskeleton of fibroblasts. J. Cell Biol. **121:**1299–1310.
60. **Nishikura, K., and J. M. Murray.** 1987. Antisense RNA of proto-oncogene c-*fos* blocks renewed growth of quiescent 3T3 cells. Mol. Cell. Biol. **7:**639–649.
61. **Nishimura, T., and P. K. Vogt.** 1988. The avian cellular homolog of the oncogene jun. Oncogene **3:**659–663.
62. **Nishina, H., T. Sato, M. Suzuki, M. Sato, and H. Iba.** 1990. Isolation and characterization of fra-2, an additional member of the fos gene family. Proc. Natl. Acad. Sci. USA **87:**3619–3623.
63. **Ozanne, B. W., R. J. Fulton, and P. L. Kaplan.** 1980. Kirsten murine sarcoma virus transformed cell lines and a spontaneously transformed rat cell line produce transforming factors. J. Cell. Physiol. **105:**163–180.
64. **Rapp, U. R., J. Troppmair, T. Beck, and M. J. Birrer.** 1994. Transformation by Raf and other oncogenes renders cells differentially sensitive to growth inhibition by a dominant negative c-*jun* mutant. Oncogene **10:**3493–3498.
65. **Riabowol, K. T., R. J. Vosatka, E. B. Ziff, N. J. Lamb, and J. B. Feramisco.** 1988. Microinjection of *fos*-specific antibodies blocks DNA synthesis in fibroblast cells. Mol. Cell. Biol. **8:**1670–1676.
66. **Rollins, B. J., E. D. Morrison, and C. D. Stiles.** 1988. Cloning and expression of *JE*, a gene inducible by platelet-derived growth factor and whose product has cytokine-like properties. Proc. Natl. Acad. Sci. USA **85:**3738–3742.
67. **Ryder, K., and D. Nathans.** 1988. Induction of proto-oncogene c-jun by serum growth factors. Proc. Natl. Acad. Sci. USA **85:**8464–8467.
68. **Ryder, K., A. Lanahan, E. Perez-Albuerne, and D. Nathans.** 1989. Jun D: a third member of the Jun gene family. Proc. Natl. Acad. Sci. USA **86:**1500–1503.
69. **Saez, E., S. E. Rutberg, E. Mueller, H. Oppenheim, J. Smoluk, S. H. Yuspa, and B. M. Spiegelman.** 1995. c-*fos* is required for malignant conversion of skin tumours. Cell **82:**721–732.
70. **Sambrook, J., E. F. Fritsch, and T. Maniatis.** 1989. Molecular cloning: a laboratory manual, 2nd. ed. Cold Spring Harbor Laboratory Press, Cold Spring Harbor, N.Y.
71. **Schlingensiepen, K.-H., R. Schlingensiepen, M. Kunst, I. Klinger, W. Gerdes, W. Seifert, and W. Brysch.** 1993. Opposite functions of *jun*-B and c-*jun* in growth regulation and neuronal differentiation. Dev. Genet. **14:**305–312.
72. **Schonthal, A., P. Herrlich, H. J. Rahmsdorf, and H. Ponta.** 1988. Requirement for *fos* gene expression in the transcriptional activation of collagenase

by other oncogenes and phorbol esters. Cell **54:**325–334.
73. **Sherman, L., J. Sleeman, P. Herrlich, and H. Ponta.** 1994. Hyaluronate receptors: key players in growth, differentiation, migration and tumor progression. Curr. Opin. Cell Biol. **6:**726–733.
74. **Smith, M. R., S. J. DeGudicibus, and D. W. Stacey.** 1986. Requirement for c-ras proteins during viral oncogene transformation. Nature **320:**540–543.
75. **St. John, T., J. Meyer, R. Idzerda, and W. M. Gallatin.** 1990. Expression of CD44 confers a new adhesive phenotype on transfected cells. Cell **60:**45–52.
76. **Suzuki, T., M. Murakami, N. Onai, E. Fukada, Y. Hashimoto, M. H. Sonobe, T. Kameda, M. Ichinose, K. Miki, and H. Iba.** 1994. Analysis of AP-1 function in cellular transformation pathways. J. Virol. **68:**3527–3535.
77. **Takeuchi, K., N. Sato, H. Kasahara, N. Funayama, A. Nagafuchi, S. Yonemura, S. Tsukita, and S. Tsukita.** 1994. Perturbations of cell adhesion and microvilli formation by antisense oligonucleotides to ERM family members. J. Cell Biol. **125:**1371–1384.
78. **Tanaka, Y., D. H. Adams, S. Hubscher, H. Hirano, U. Siebenlist, and S. Shaw.** 1993. T-cell adhesion induced by proteoglycan-immobilizes cytokine MIP-1β. Nature **361:**79–82.
79. **Thomas, L., T. Etoh, I. Stamenkovic, M. C. Mihm, and R. H. Byers.** 1993. Migration of human melanoma cells on hyaluronate is related to CD44 expression. J. Invest. Dermatol. **100:**115–120.
80. **Tomsak, J., and E. Haye.** 1984. Analysis of the role of microfilaments and microtubules in acquisition of the bipolarity and elongation of fibroblasts in hydrated collagen gels. J. Cell Biol. **99:**536–549.
81. **Troen, B. R., S. S. Chauhan, D. Ray, and M. M. Gottesman.** 1991. Downstream sequences mediate induction of the mouse cathepsin L promoter by phorbol esters. Cell Growth Differ. **2:**23–31.
82. **Tsukita, S., K. Oishi, N. Sato, J. Sagara, A. Kawai, and S. Tsukita.** 1994. ERM family members as molecular linkers between the cell surface glycoprotein CD44 and actin-based cytoskeletons. J. Cell Biol. **126:**391–401.
83. **Underhill, C. B., and B. P. Toole.** 1981. Receptors for hyaluronate on the surface of parent and virus-transformed cell lines: binding and aggregation studies. Exp. Cell Res. **131:**419–423.
84. **Van Beveren, C., S. Enami, T. Curran, and I. M. Verma.** 1984. FBR murine osteosarcoma virus. 11. Nucleotide sequence of the provirus reveals that the genome contains sequences acquired from two cellular genes. Virology **135:** 229–243.
85. **Weber, G., S. Ashkar, M. Glimcher, and H. Cantor.** 1996. Receptor-ligand interaction between CD44 and osteopontin. Science **271:**509–512.
86. **Zerial, M., R. Toschi, R. P. Ryseck, M. Schuermann, R. Muller, and R. Bravo.** 1989. The product of a novel growth factor activated gene, fosB, interacts with Jun proteins enhancing their DNA binding activity. EMBO J. **8:**805–813.